IEEE Access
Multidisciplinary | Rapid Review | Open Access Journal

Received October 13, 2021, accepted November 2, 2021, date of publication November 4, 2021, date of current version November 11, 2021.

Digital Object Identifier 10.1109/ACCESS.2021.3125445

Antenna System for Communication in Underground Mining Environment to Ensure Miners Safety

KAPIL GANGWAR[1], (Graduate Student Member, IEEE), GARY CHIEN-YI CHEN[1], KEVIN KHEE-MENG CHAN[1], (Member, IEEE), RAVI KUMAR GANGWAR[2], (Senior Member, IEEE), AND KARUMUDI RAMBABU[1], (Member, IEEE)

[1]Department of Electrical and Computer Engineering, University of Alberta, Edmonton, AB T6G 1H9, Canada
[2]Department of Electronics Engineering, Indian Institute of Technology (Indian School of Mines) Dhanbad, Dhanbad, Jharkhand 826004, India

Corresponding author: Kapil Gangwar (kgangwar@ualberta.ca)

ABSTRACT Miniaturized antenna system for the safety of miners in an underground mine for providing communication has been presented in this paper. Miniaturization of the proposed antennas is achieved by using printed inverted-F and inverted-L elements. The impedance bandwidth of the proposed antenna geometry for GSM application is over 16%. Measured and simulated characteristics of the antenna agree very well. The measured gain of the antenna, with a two-director, is over 4.98 dBi when mounted on a ground plane and around 5.2 dBi when placed on the wall of an underground mine. Proper placement of the antenna in the mine environment is discussed for better communication for miners. Experimental validation of the antenna system is performed in a real underground mine. The radiation performance of the system is also studied in the mine environment. The proposed antenna may be suitable for establishing communication in underground mines to ensure the safety of miners.

INDEX TERMS Mining industry safety, mining industry, wireless base station antennas.

I. INTRODUCTION

Miniaturized antenna designs for the application of wireless communications in mining industries have attracted the attention of engineers all over the world. Generally, antenna miniaturization is essential for handset designs. However, broadband miniaturized base station antenna designs are in great demand for cellular and data transfer applications in the underground mining industry. Due to the non-line-of-sight and incompatible environment, wireless communication inside the mine is very challenging. Due to the harsh environmental conditions and risk of fire casualties, communication through telephones interlinked by thick plastic-coated cables is still availed in the mining industry. Miner's safety, productivity, and maintenance of a smooth working environment are some important aspects that the coal mines should ensure. During a disaster, miners can be trapped inside the mining area as cables cannot withstand such high pressures [1], [2]. The need of the hour is to establish a reliable, proper, and efficient way of communication from the working area to the surface to track the miners during rescue operations, thereby removing disruptive trailing wires. There are three main frequencies band for coal mine communication (VHF/UHF/SHF) governed by mines safety and health administration ranging from 150 MHz to 6 GHz. High-frequency signals suffer severe attenuation than the lower frequency signals while propagating in the same environment. Line of sight communication is obstructed due to complex and non-symmetric mine structures. Due to power restrictions on gadgets and high attenuation of the signal, restricted wireless applications are performed in the mining area. Therefore, the demand for miniaturized, high-gain broadband antennas has increased in mining areas. Coal metal underground mines have passways that range up to 500m-1km with 4-5 m width and 3-3.5 m height responsible for ventilation and transportation purposes. Generally, from the main entries, the crosscut at right angles is installed at every 20 m of distance [3]–[5]. Former measurement shows that the

The associate editor coordinating the review of this manuscript and approving it for publication was Lorenzo Ciani.

propagation of RF signals strongly depends on underground mine properties.

In [6], an EBG-backed flexible printed Yadi-Uda Antenna is proposed for industrial, scientific, and medical radio bands. The operating frequency of this antenna is 2.4 GHz. In [7], a pattern reconfigurable Yagi-Uda antenna with linear polarization is proposed for WiMAX applications. The proposed structure shows a stable radiation pattern at 3.6 GHz. An Integrated Yagi-Uda is presented in [8] with tapered printed Yagi as the primary feeder. The antenna is resonating at a center frequency of 9.1 GHz applicable for commercial wireless LAN and satellite communication. In [9], a low-profile planar Yagi-Uda antenna having I-shaped resonators is presented which can be used for satellite communication and wireless LAN applications. The antenna has an operating frequency centered at 6.5 GHz. A printed Quasi-Yagi antenna employing monopole elements is proposed [10] applicable for Bluetooth, Wi-Fi, and mobile communication. The antenna operates at a center frequency of 2.04 GHz. In [11], a compact nonreciprocal Yagi-Uda antenna is proposed which can be applied in communication, sensing, and radar systems. The antenna operates at the center frequency of 2.4 GHz. Table 1 shows the comparison of the proposed antenna with other relevant published work.

TABLE 1. Comparison of the proposed antenna with other relevant work.

	Frequency (GHz)	Antenna size	Gain (dBi)	Application
[6]	2.4	$1.08\lambda_o$x $1.08\lambda_o$	8.53	Industrial, scientific medical radio band
[7]	3.6	$0.903\lambda_o$x $0.843\lambda_o$	5.84	WiMAX
[8]	9.1	$4.50\lambda_o$ x $1.00\lambda_o$	18	Commercial Wireless LAN, Satellite Communication
[9]	6.5	$1.70\lambda_o$x $1.20\lambda_o$	10	Satellite Communication
[10]	2.04	$0.51\lambda_o$ x $0.57\lambda_o$	4.56	Bluetooth, Wi-Fi, Mobile communication
[11]	2.4	$1.36\lambda_o$ x $0.64\lambda_o$	4	Radar, sensing systems
Pro. ant.	**0.9**	$\mathbf{0.675\lambda_o}$ **x** $\mathbf{0.171\lambda_o}$	**4.98**	**GSM band**

In [12], a high gain bidirectional antenna is presented, which is appropriate for wireless communication in coal mines. The antenna is resonating at 2.4 GHz. The dimension is around $2.4\lambda_o \times 0.128\lambda_o$. In [13], a compact array element is employed for a coal mine communication. The antenna shows bidirectional end-fire radiation pattern characteristics. The array is operating at GSM900 with a bandwidth of 7.5% and a gain of around 8.5 dBi. The dimension of the array is about $2.5\lambda_o \times 0.30\lambda_o$. Coplanar fed C- shaped slot antenna array is presented in [14] for coal mining communication. The antenna operates at 2.4 GHz with a maximum gain of around 10 dBi. The dimensions of the array antenna are $4\lambda_o \times 0.80\lambda_o$. In [15], a two-way directional antenna is presented for underground mine-tunnel communication at 2.4 GHz with a bandwidth of 14%. The antenna has gain value of 8.35 dBi having dimension of $1.84\lambda_o \times 0.17\lambda_o$. In [16], reconfigurable antenna for improved communication in underground mines is proposed. The antenna is operating at 2.45 GHz with a bandwidth of 16.3 % and a gain of 5.25 dBi. The antenna is circular having a diameter of $0.82\lambda_o$. A small hemicylindrical-shaped antenna in [17] is presented for underground mine communication. The antenna operates at 58.27 MHz with a maximum gain of around 3.43 dBi and bandwidth of 0.506%. The dimensions of the array antenna are $0.038\lambda_o \times 0.035\lambda_o$. In [18], a dual-band antenna is proposed using a genetic algorithm for underground mining communication. The antenna is operating at 2.45 GHz and 5.8 GHz with a gain of 8.06 dBi and 7.35 dBi respectively. The total size of the antenna is $1.15\lambda_o \times 1.15\lambda_o$. In [19], a circularly polarized antenna is employed for the Radiofrequency identification tag applicable for underground localization systems. The antenna is operating at GSM900 with a bandwidth of 3.9% and a gain of around −8.5 dBi. The dimension of the antenna is about $0.60\lambda_o \times 0.60\lambda_o$.

This paper proposes a Yagi concept-based printed antenna using inverted-F and inverted-L planar structures working for the GSM frequency band which can be applicable for underground mining communication systems. The proposed antenna array configuration is influenced by the wired antenna [20] needs no feed network, and the Inverted-F antenna (IFA) with three Inverted-L elements (ILA) is smaller than the regular microstrip patch design. This design uses an inverted-F structure as an active element (feeding element) and two inverted-L structures as a director, and another inverted-L structure as a reflector. This design provides a broad bandwidth (>16%) as well as miniaturization. The feeding arrangement is simple and straightforward. Section II describes the design of the individual structure of the antenna. Section III discusses the results of the proposed antenna; IV presents the field measurements inside the mine. Section V discusses the implementation of the proposed antenna in the underground mine environment.

II. DESIGN AND ANALYSES OF THE MINIATURIZED ANTENNA

For short-range, indoor broadcasting, medical, partial discharge detection, and atmospheric parameter sensing applications, printed dipoles, microstrip patch antennas, and monopoles are ideal due to the omnidirectional radiation characteristics [21]–[23]. However, the bandwidth of the above antennas is not enough for many wireless applications.

In this paper, we propose a structural design for the antenna that comprises printed inverted-F (IFA) and inverted-L (ILA) antenna elements to achieve the desired bandwidth as well as miniaturization. These IFA and ILA are variants of a monopole. The IFA is known for its capacity to yield flexibility in impedance matching and polarization, a characteristic that is advantageous for indoor environmental conditions [24]. Fig.1 shows the proposed antenna geometry.

The antenna is printed on the substrate with a dielectric permittivity of 3.5 and a loss tangent of 0.0018. The dimensions of the proposed antenna array elements are: W1=38.71 mm, W2=65.65 mm, W3=67.09 mm, W4=38.71 mm, H1=35.52 mm, H2=26.08 mm, and H3=44.05. The gaps between elements are AF=3.74 mm, A1=1 mm, A2=1.85 mm, and A3=1 mm and D1=1.24 mm. The dimension of the substrate is HS=57.4 mm, HG=0.8 mm, and WS=175.64 mm. The antenna is mounted vertically over a large ground plane (22.5×5 cm^2).

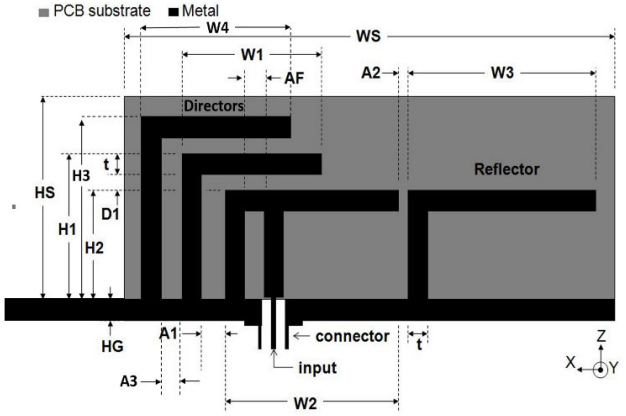

FIGURE 1. Proposed antenna configuration.

The resonant length of the IFA is the quarter wavelength in free space. The optimal length of the IFA is 8 to 10% short of its free space length, and it depends on the width of the traces of the IFA and the dielectric constant of the material that the IFA is printed. The printed IFA's input impedance is a function of height (H2), length (W2), and the gap between the feed and shorting pin (AF). To improve the performance of the IFA, mitering the corner and tapering the feed line can be accommodated in such a manner that proper current flow will be maintained. Fig.2 shows the simulated (HFSS) input impedance of the proposed antenna geometry as a function of

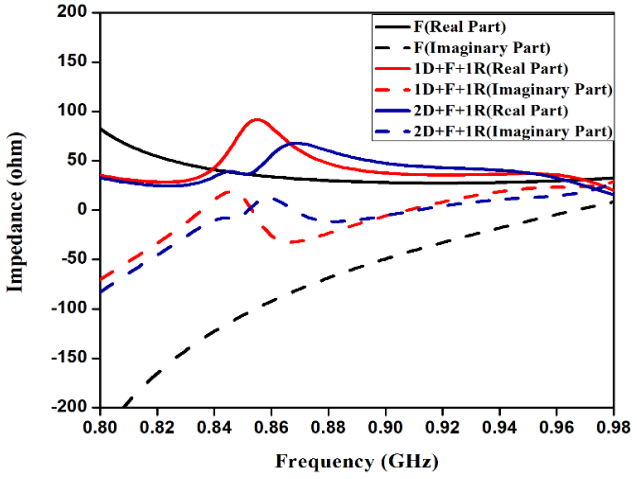

FIGURE 2. Simulated (HFSS) input impedance of the proposed antenna as a function of elements present in antenna: Only F structure, 1 F structure 1 director 1 reflector, and 1 F structure 2 directors 1 reflector.

elements present in the antenna. Normalized input impedance at 900 MHz was around 0.55-j0.98 when only Inverted-F microstrip with coaxial feed was introduced. This configuration shows very little power delivered to the antenna due to the significantly high reflection coefficient value of 0.58.

Further introduction of an inverted-L director to the antenna system increases the input impedance imaginary part because of parasitic coupling between the microstrips. Another inverted-L director, when placed adjacent to the previous director, increases the real part of input impedance by 20 ohms, resulting in the shift of the frequency band to the acceptable range (824-960 MHz). However, the power transferred to the antenna system was still poor. Further, the addition of an inverted-L reflector while removing the second director introduces the inductive coupling, consequently, reducing the input impedance's imaginary part without any change in the real part. The VSWR in this condition was found to be (<1.8), resulting in more power is accepted than in the preceding case. Again, the second director is introduced to the existing design, increasing inductive coupling further and the normalized real input impedance, which significantly decreases the amount of reflected power from the antenna. Parasitic coupling between the IFA and ILA of the proposed antenna improves impedance bandwidth. In this configuration, IFA is the active element directly fed through the microstrip or coaxial line, and ILA is mutually excited. The design of IFA and tuning it to the desired resonant frequency in the array configuration are the critical aspects of the antenna design. Implementation of Short-circuited stub plays an important role in compensation of capacitance in the array's input impedance which is introduced by parallel section of the IFA. The wider traces can enhance the achievable bandwidth of the IFA. The typical *VSWR* bandwidth of an IFA for a trace width (t) of 8.2 mm is 9 %. The input resistance of the IFA can be controlled through the gap between the ground plane and horizontal section, as well as the gap between the feed and the shorting post. The broadband characteristics are achieved by optimizing the array parameters.

The length of the ILA that acts as a director in the proposed antenna should be shorter than the quarter wavelength so that it will be more capacitive than IFA. Similarly, the length of the ILA that acts as a reflector should be longer than the quarter wavelength so that it will be more inductive than IFA [25]. It is known that the input impedance of the active element in the array decreases due to the parasitic elements [26]. Therefore, the input impedance of stand-alone IFA in the proposed antenna is chosen intentionally higher than 50 Ω to accommodate the parasitic elements and avoid the impedance matching circuit. In this configuration director strongly couples with the active element; hence the design is more sensitive towards the director. Fig.3 shows the simulated return loss (S11) of the antenna for the following design evolution process from only one F structure to one F structure two directors one reflector. This design covers the entire bandwidth of the GSM 900 standard, i.e., from 824 MHz to 960 MHz.

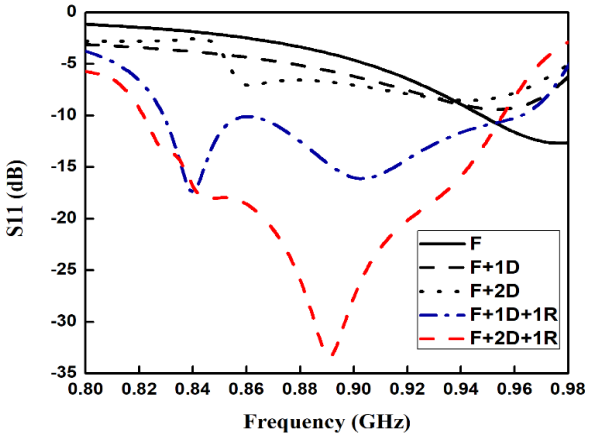

FIGURE 3. Simulated (HFSS) S11 of the proposed antenna as a function of elements present in antenna: Only F structure,1 F structure 1 director,1 F structure 2 directors,1 F structure 1 director 1 reflector, and 1 F structure 2 directors 1 reflector.

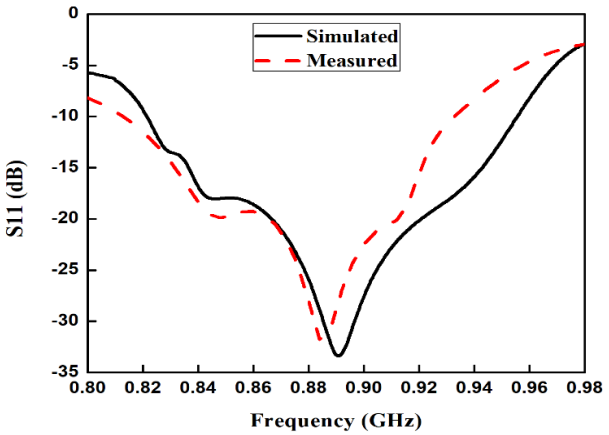

FIGURE 4. S11 of the antenna on the large ground: measured (red dash line), simulation (black solid line).

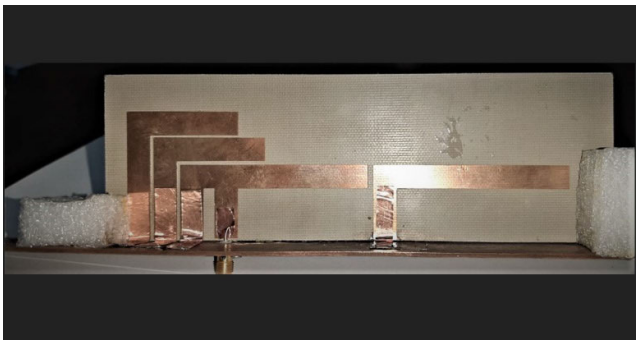

FIGURE 5. Photo of the fabricated antenna for GSM band (824 – 960 MHz).

The bandwidth achieved for the proposed antenna is over 17% for VSWR is 2:1.

The radiation characteristics of the IFA are the vectorial sum of the radiated fields by IFA and its image due to the ground plane. The combination of IFA and its image behaves as an asymmetric dipole due to the narrow ground plane; hence radiation pattern will not be symmetric. The radiation characteristics of the proposed antenna depend on the current over the array elements and their images. At lower frequencies of the band, radiation is truly unidirectional. A minimum of 5 dB differences in the front-to-back ratio is observed on most of the bandwidth. Therefore, the antenna will be mounted on the wall towards the reflector end, i.e., minimum radiation direction. By adding more directors to the antenna configuration, the gain and front-to-back ratio of the antenna can be improved.

III. ANTENNA MEASUREMENT

The proposed antenna for the GSM band is developed, by placing it on a large ground plane, based on the design parameters presented in section II. Fig.4 shows the measured and simulated results for return loss (S11) of the proposed antenna. The agreement between the simulation and measurement is quite convincing. This design covers the full GSM band, i.e., between 824 MHz to 960 MHz. The fabricated antenna design is shown in Fig.5. In this design, the ground plane is extended more towards the director of the antenna due to the high current density on the ground plane near the director and feed element of the array.

Antenna performance is diminished by reducing the ground plane size as the currents are distorted on the ground plane. The measured bandwidth of the antenna is slightly lower than the simulated bandwidth; however, the measured bandwidth covers the required GSM bandwidth. The shift in the measured return loss of the fabricated antenna is due to the reactance introduced by the ridge of copper tape at the end of the ground plane.

The ground plane of the fabricated antenna was built by taping the bottom and top layers of a piece of PCB board instead of solid metal. Fig.6(a) and Fig.6(b) show the measured and simulated co-pol and cross-pol radiation pattern of the proposed antenna in the E plane and H-plane respectively at 900 MHz.

Patterns show omnidirectional characteristics in the end-fire direction. This type of pattern is suited for wall mount support in which the main beam stems away from the supporting structure. Therefore, this design can accommodate any real-time application scenarios, such as mounting the antenna on a small or large ground plane.

It is shown that radiation in all the simulations and measured patterns in the elevation plane are squinted. One of the main reasons for the squinted radiation pattern is the image of the antenna due to the ground plane. This squinted pattern may be used to the advantage, to focus the energy while mounting the antenna to the roof of a building. Fig.6(c) and Fig.6(d) shows a 3-D radiation pattern and Current distribution at 900 MHz. Radiation patterns of the antenna are more omnidirectional in the azimuth plane and radiation peaks at 15 degrees in the elevation plane.

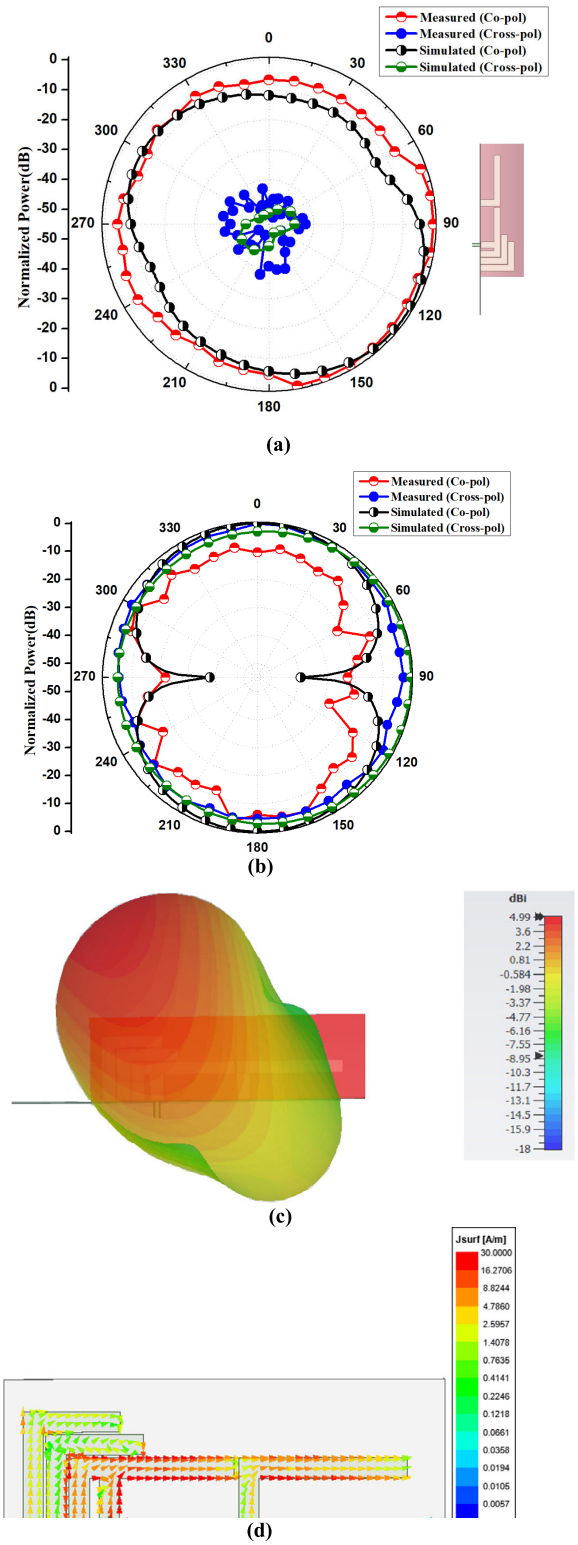

FIGURE 6. Measured and simulated radiation pattern of the proposed antenna (a) E-plane (b) H-plane; (c)3-D radiation pattern (d) Current distribution at 900 MHz.

Fig.7 shows the plot of maximum gain over the operating GSM band frequency. The measured gain of the antenna with the large ground plane is over 4.5 dBi on the entire frequency band in an anechoic chamber.

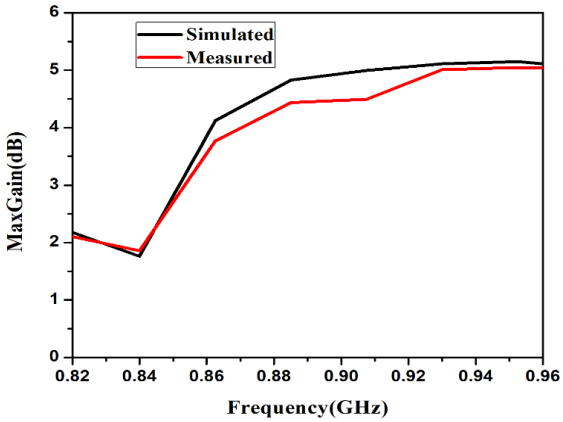

FIGURE 7. Maximum gain as a function of frequency for GSM band.

IV. MEASUREMENT INSIDE THE MINE

To validate the performance of the antenna system in the underground mine environment, measurement is performed in UCIL Narwapahar mine, Jharkhand India. The passway of the mines was 5 × 4 m^2 with a height of around 3 meters. In the measurement setup, the transmitter is fixed at one position, and the receiver is moved to 9 different locations in the vicinity of the coal mine environment, as shown in Fig.8.

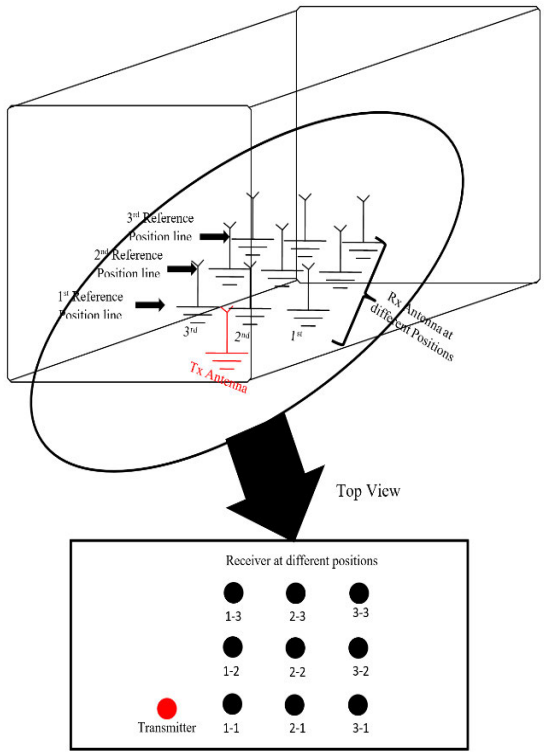

FIGURE 8. Antenna measurement setup in the mine environment.

S_{21} is measured concerning the three reference positions. Fig.9 shows the measurement setup of the two similar fabricated antennas. Fig.10, Fig.11, and Fig.12 show the measurement result of the 1st, 2nd, and 3rd reference positions

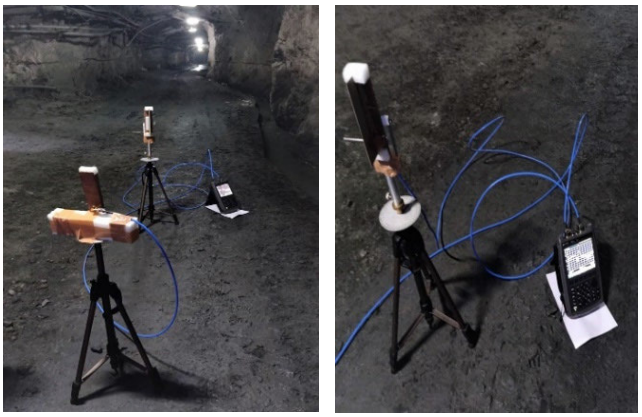

FIGURE 9. Photo of the measurement setup of the fabricated antenna in underground mine.

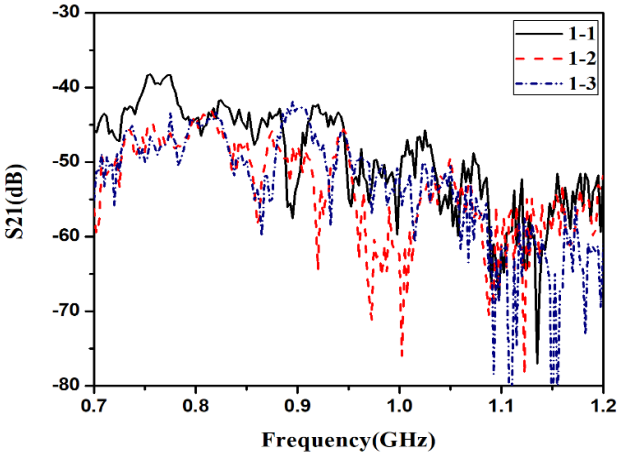

FIGURE 10. Measurement result of 1st Reference position.

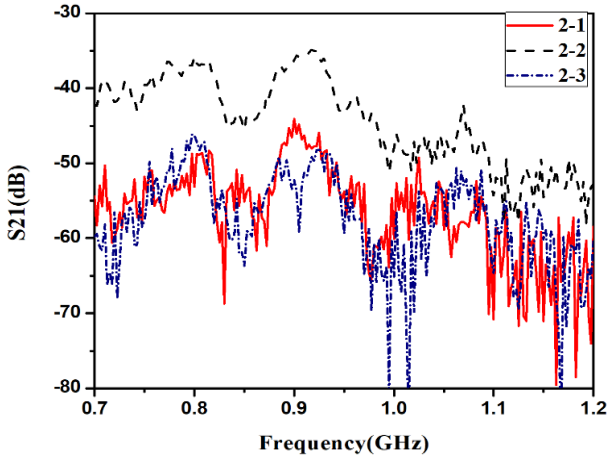

FIGURE 11. Measurement result of 2nd Reference position.

concerning the transmitter antenna fixed at one position. The graphs depict the amount of power transmitted by the antenna deteriorating as the receiver moves away from the transmitter. According to Friis transmission equation, pass loss can be

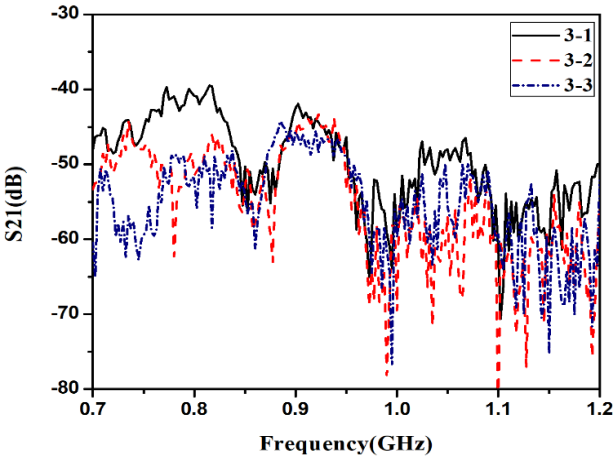

FIGURE 12. Measurement result of 3rd Reference position.

determined under ideal conditions when the power delivered, power received, a gain of two antennas separated by some distance is known [27]. Since the measurement is done in the underground mine, an additional loss will come into effect.

$$P_{rec}(dBm) = P_{trans}(dBm) + G_{rec}(dB) + G_{trans}(dB) - L_{freespace}(dB) - L_{mine}(dB) \quad (1)$$

Equation (1) shows the single-path channel model where P_{rec} and P_{trans} are received and transmitted powers, G_{rec} and G_{trans} are the gain value of receiving and transmitting antenna respectively. $L_{freespace}\,(dB)$ and $L_{mine}(dB)$ are the free space path loss and loss caused by the underground mine environment respectively.

$$L_{freespace}\,(dB) = 20\log\,(f\,(MHz)) + 20\log\,(x(m)) - 27.55 \quad (2)$$

$$S_{21}\,(dB) = P_{rec}\,(dBm) - P_{trans}\,(dBm) - 30 \quad (3)$$

$L_{freespace}$ in dB can be determined [28] using equation (2) where f is the frequency of operation in MHz, x is the distance in meters from transmitter to receiver. The value of $P_{rec} - P_{trans}$ at each location can be obtained from measured S_{21} shown in fig. 10, fig.11, and fig.12 at 900 MHz. The value of L_{mine} at 9 different locations can be computed using equations (1), (2), and (3). Fig.13 shows the loss value caused due to the underground mine environment at different locations of the receiver at 900 MHz. It can be concluded that the amount of power transmitted by the antenna deteriorates as the receiver moves away from the transmitter.

Fig.14 shows the Far-field pattern inside the mine and anechoic chamber at 900 MHz. The radiation pattern inside the mine shows nearly omnidirectional characteristics but is somewhat distorted because of the environmental condition and losses inside the mine as compared to the suitable environment for an antenna in the anechoic chamber.

Since the measurement results of the antenna system are quite convincing and show good performance in a real underground mine environment. So, the idea of proper placement of

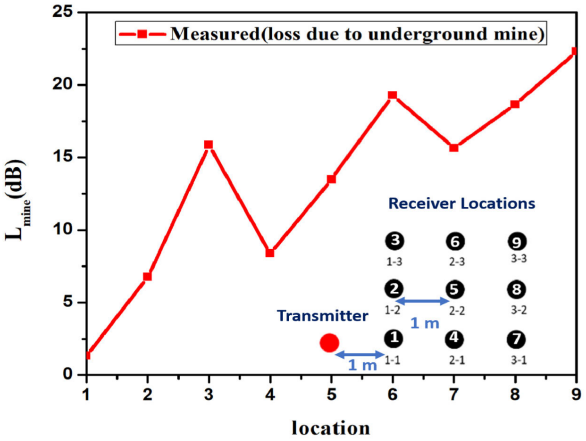

FIGURE 13. Loss value(dB) caused due to the underground mine environment at different locations of the receiver at 900 MHz.

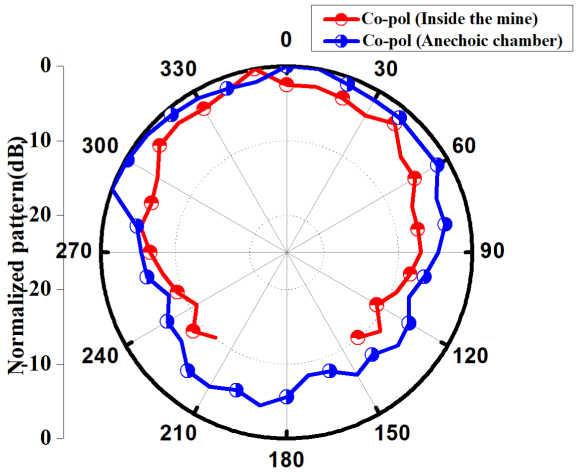

FIGURE 14. The far-field pattern inside the mine and anechoic chamber at 900 MHz.

the proposed antenna system as illustrated in the next section can be efficiently used in the mining industry for the miner's safety resulting in a reliable, proper, and efficient way of wireless communication prevailing the disruptive telephonic wire.

V. IMPLEMENTATION IN MINE ENVIRONMENT

A cuboidal mine environment structure is created in CST Microwave studio with a size $5 \times 3 \times 3$ m^3 loaded with a dielectric constant of 2.6, having a loss tangent of 0.17. In the simulation, the antenna is mounted at the corner of the underground mine wall in a 90-degree orientation, as shown in Fig.15. First, simulation is performed by taking just one wall at which the antenna is mounted, and the result is recorded, followed by all four walls of mine structure.

Since the radiation peak of the antenna is radiating at 15 degrees, placing the antenna on the coal wall in the orientation has provided an advantage of radiating power distribution in the area of interest. A miner with a height of 1.8 m or so,

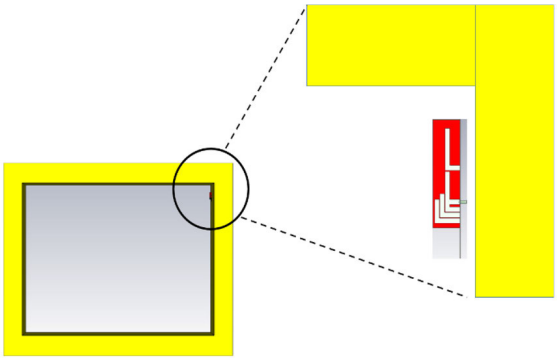

FIGURE 15. Configuration of the antenna mounted on mine wall (90-degree orientation).

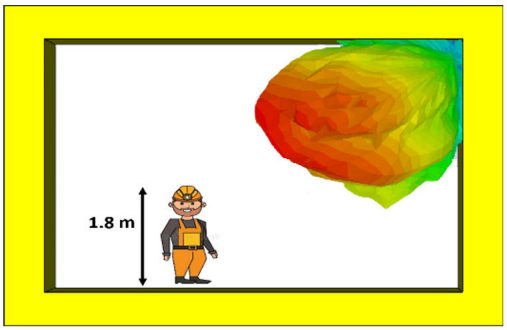

FIGURE 16. The 3-D radiation pattern of the antenna mounted on the mine wall(90-degree orientation).

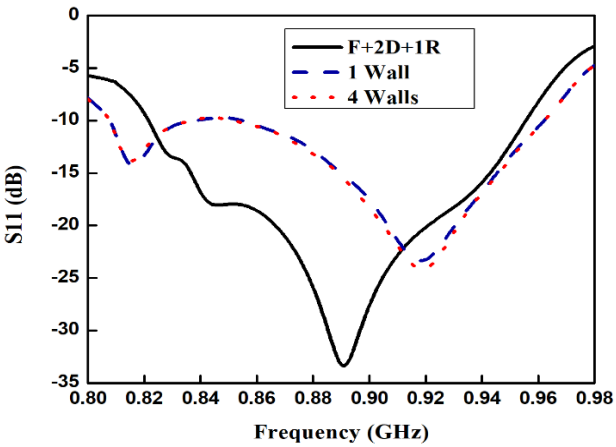

FIGURE 17. Reflection coefficient as a function of frequency for proposed antenna and antenna placed on the wall.

walking with a receiver on head or hand, can easily receive the signal from the transmitter. The miner can be easily tracked in case of an emergency as the antenna in sensing mode will always monitor the real-time movement and will send the signal to the base station.

The 3-D radiation pattern at 900 MHz is shown in Fig.16 when the antenna is mounted at the corner. Fig.17 shows the

TABLE 2. Comparison of the proposed antenna with another antenna used for underground mine communication.

	Frequency (GHz)	Antenna size	Gain(dBi)	BW (%)
[12]	2.4	2.4 λ_o x 0.128 λ_o	2.4	12.08
[13]	0.9	2.5 λ_o x 0.30 λ_o	8.5	7.5
[14]	2.4	4 λ_o x 0.80 λ_o	10	9.58
[15]	2.4	1.84λ_ox 0.17λ_o	8.35	14.0
[16]	2.45	0.82λ_ox 0.82λ_o	5.25	16.3
[17]	0.058	0.038λ_o x 0.035λ_o	3.43	0.506
[18]	2.4/5.8	1.15λ_ox 1.15λ_o	8.06/7.35	3.50/2.15
[19]	0.9	0.60λ_o x 0.60λ_o	-8.5	3.9
Proposed antenna	**0.9**	**0.675λ_o x 0.171λ_o**	**4.98**	**17.0**

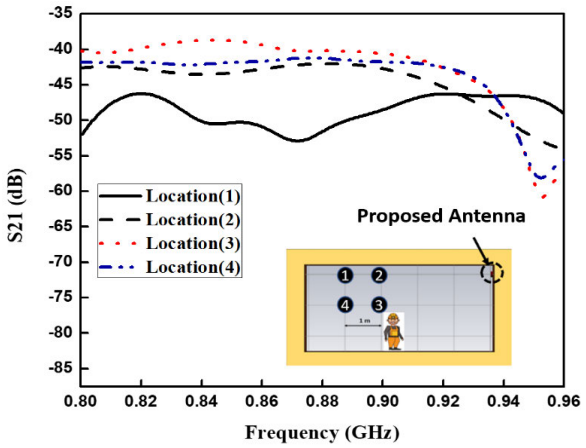

FIGURE 18. S21 as a function of frequency at locations 1,2,3 and 4 from proposed antenna placed on one side of coal wall.

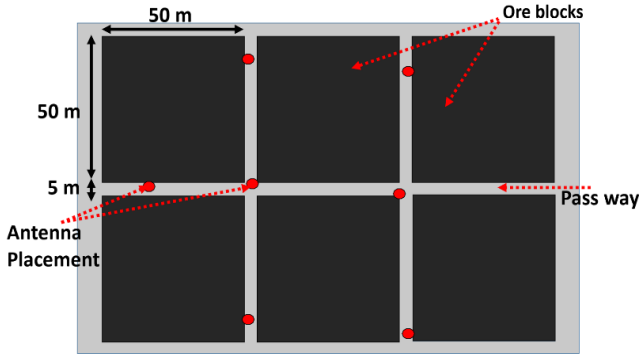

FIGURE 19. Antenna placement planning in the underground mine environment.

reflection coefficient of the proposed antenna placed in the presence of only one wall and all four walls. The simulation is performed with a similar antenna acting as a receiver at locations 1, 2,3, and 4. S21 is determined as shown in Fig.18.

S21 curves exhibit an idea about the power received by the antenna when moving from locations 1 to 4. Considering all the factors of antenna performance and mining environment, one of the suitable placement planning of the proposed antenna can be as shown in fig.19. Table 2 shows the comparison of the proposed antenna with another antenna used for underground mine communication.

VI. CONCLUSION

This paper discusses a miniaturized antenna for miners' safety in underground mining communication systems. The achievable bandwidth of the antenna is over 16%, and the gain is over 2.5 dBi. The gain of the antenna is over 4.5 dBi while mounted on a large ground plane. The radiation pattern in the azimuth plane is almost symmetric; however, the radiation pattern in the elevation plane shows distortion due to the image currents on the ground plane. This proposed antenna also provides unidirectional radiation; hence this antenna can be mounted on walls of coal mines to get the radiation in the area where the miners are walking. When mounted on the coal wall, the radiation pattern of the antenna depicts that the power is allocating in the interested area. Hence, the antenna can be efficiently used and placed in the vicinity of the underground mine environment for communication purposes at the GSM band.

ACKNOWLEDGMENT

The authors are thankful to the entire administration of UCIL (Jaduguda Group of Mines, Narwa Pahar, Jharkhand, India) especially Manoj Kumar, Rakesh Kumar, and Dr. P. K. Adhikari for their support to conduct the experiment. They are also thankful to Kundan Kumar Suman and Rahul Kumar, IIT (ISM) Dhanbad for their help to measure the radiation patterns.

REFERENCES

[1] L. K. Bandyopadhyay *et al.*, "Radio frequency communication system in underground mines," in *Proc. 28th Int. Seminar General Assembly Int. Union Radio Sci. (URSI)*, New Delhi, India, Oct. 2005.

[2] D. Large, L. Ball, and A. Farstad, "Radio transmission to and from underground coal mines-theory and measurement," *IEEE Trans. Commun.*, vol. COM-21, no. 3, pp. 194–202, Mar. 1973.

[3] R. Jacksha and C. Zhou, "Measurement of RF propagation around corners in underground mines and tunnels," *Transactions*, vol. 340, no. 1, pp. 30–37, Jan. 2016, doi: 10.19150/trans.7324.

[4] H. Sacks and R. Chufo, "Medium-frequency propagation in coal mines," in *Proc. 4th WVU Conf. Coal Mine Electrotechnol.* Morgantown, WV, USA: West Virginia Univ., Aug. 1978, pp. 27.1–27.12.
[5] C. A. Balanis, J. L. Jeffrey, and Y. K. Yoon, "Electrical properties of eastern bituminous coal as a function of frequency, polarization and direction of the electromagnetic wave, and temperature of the sample," *IEEE Trans. Geosci. Electron.*, vol. GE-16, no. 4, pp. 316–323, Oct. 1978.
[6] B. S. Abirami and E. F. Sundarsingh, "EBG-backed flexible printed Yagi–Uda antenna for on-body communication," *IEEE Trans. Antennas Propag.*, vol. 65, no. 7, pp. 3762–3765, Jul. 2017, doi: 10.1109/TAP.2017.2705224.
[7] S. Gaya, R. Hussain, M. S. Sharawi, and H. Attia, "Pattern reconfigurable Yagi–Uda antenna with seven switchable beams for WiMAX application," *Microw. Opt. Technol. Lett.*, vol. 62, no. 3, pp. 1329–1334, Mar. 2020, doi: 10.1002/mop.32147.
[8] M. Nasir, Y. Xia, M. Jiang, and Q. Zhu, "A novel integrated Yagi–Uda and dielectric rod antenna with low sidelobe level," *IEEE Trans. Antennas Propag.*, vol. 67, no. 4, pp. 2751–2756, Apr. 2019, doi: 10.1109/TAP.2019.2897478.
[9] Z. Yang, L. Zhang, and T. Yang, "A microstrip magnetic dipole Yagi–Uda antenna employing vertical I-shaped resonators as parasitic elements," *IEEE Trans. Antennas Propag.*, vol. 66, no. 8, pp. 3910–3917, Aug. 2018, doi: 10.1109/TAP.2018.2835673.
[10] A. D. Chaudhari and K. P. Ray, "Printed broadband quasi-Yagi antenna with monopole elements," *IET Microw., Antennas Propag.*, vol. 14, no. 6, pp. 468–473, May 2020, doi: 10.1049/iet-map.2019.0628.
[11] J. Zang, X. Wang, A. Alvarez-Melcon, and J. S. Gomez-Diaz, "Nonreciprocal Yagi–Uda filtering antennas," *IEEE Antennas Wireless Propag. Lett.*, vol. 18, no. 12, pp. 2661–2665, Dec. 2019, doi: 10.1109/LAWP.2019.2947847.
[12] W. Liu, Z. Zhang, Z. Tian, and Z. Feng, "A bidirectional high-gain cascaded ring antenna for communication in coal mine," *IEEE Antennas Wireless Propag. Lett.*, vol. 12, pp. 761–764, 2013, doi: 10.1109/LAWP.2013.2270936.
[13] L. Liu, Z. Zhang, Z. Tian, and Z. Feng, "A bidirectional endfire array with compact antenna elements for coal mine/tunnel communication," *IEEE Antennas Wireless Propag. Lett.*, vol. 11, pp. 342–345, 2012, doi: 10.1109/LAWP.2012.2191383.
[14] Y. Zhao, Z. Zhang, and Z. Feng, "Design of a CPW-FED C-shaped slot array antenna for coal mine/tunnel applications," *Microw. Opt. Technol. Lett.*, vol. 55, no. 8, pp. 1784–1789, Aug. 2013, doi: 10.1002/mop.27695.
[15] S. B. Amo, A. Acakpovi, N. Y. Asabere, R. Abubakar, and R. Sowah, "High gain 2.4 GHz two-way direction Wi-Fi antenna for underground mine-tunnel," in *Proc. IEEE 7th Int. Conf. Adapt. Sci. Technol. (ICAST)*, Aug. 2018, pp. 1–9, doi: 10.1109/ICASTECH.2018.8506823.
[16] H. Kunsei, K. S. Bialkowski, M. S. Alam, and A. M. Abbosh, "Improved communications in underground mines using reconfigurable antennas," *IEEE Trans. Antennas Propag.*, vol. 66, no. 12, pp. 7505–7510, Dec. 2018, doi: 10.1109/TAP.2018.2869250.
[17] J. C. Dash, K. Nagalakshmaiah, G. S. Reddy, and J. Mukherjee, "Electrically small hemi-cylindrical-shaped multilayered very high frequency antenna for underground mine communication," *IET Microw., Antennas Propag.*, vol. 14, no. 6, pp. 491–497, May 2020, doi: 10.1049/iet-map.2019.0744.
[18] Y. B. Chaouche, M. Nedil, I. B. Mabrouk, and M. Belazzoug, "A dual-band antenna backed by AMC surface using genetic algorithm for 2.4/5.8 GHz underground mining communications," in *Proc. IEEE Int. Symp. Antennas Propag. North Amer. Radio Sci. Meeting*, Jul. 2020, pp. 929–930, doi: 10.1109/IEEECONF35879.2020.9330406.
[19] Y. Chen and A. Z. Elsherbeni, "Circularly polarized RFID tag antenna design for underground localization system," in *Proc. United States Nat. Committee URSI Nat. Radio Sci. Meeting (USNC-URSI NRSM)*, 2021, pp. 205–206, doi: 10.23919/USNC-URSINRSM51531.2021.9336514.
[20] G. Chen, K. K.-M. Chan, and K. Rambabu, "Miniaturized Yagi class of antennas for GSM, WLAN, and WiMAX applications," *IEEE Trans. Consum. Electron.*, vol. 56, no. 3, pp. 1235–1240, Aug. 2010, doi: 10.1109/TCE.2010.5606252.
[21] W. Wang, X.-W. Xuan, W.-Y. Zhao, and H.-K. Nie, "An implantable antenna sensor for medical applications," *IEEE Sensors J.*, vol. 21, no. 13, pp. 14035–14042, Jul. 2021, doi: 10.1109/JSEN.2021.3068957.
[22] J.-H. Low, P.-S. Chee, and E.-H. Lim, "Deformable liquid metal patch antenna for air pressure detection," *IEEE Sensors J.*, vol. 20, no. 8, pp. 3963–3970, Apr. 2020, doi: 10.1109/JSEN.2019.2961514.
[23] G. V. R. Xavier, E. G. da Costa, A. J. R. Serres, L. A. M. M. Nobrega, A. C. Oliveira, and H. F. S. Sousa, "Design and application of a circular printed monopole antenna in partial discharge detection," *IEEE Sensors J.*, vol. 19, no. 10, pp. 3718–3725, May 2019, doi: 10.1109/JSEN.2019.2896580.
[24] Y.-W. Jang and S. W. Lee, "A multi-band inserted Yagi-type arrayed-slots PIFA antenna using a large offset rectangular L-shaped feed," *Microw. J.*, vol. 51, no. 1, p. 126, Jan. 2008.
[25] C. Soras, M. Karaboikis, G. Tsachtsiris, and V. Makios, "Analysis and design of an inverted-F antenna printed on a PCMCIA card for the 2.4 GHz ISM band," *IEEE Antennas Propag. Mag.*, vol. 44, no. 1, pp. 37–44, Feb. 2002.
[26] C. A. Chen and D. K. Cheng, "Optimum element lengths for Yagi–Uda arrays," *IEEE Trans. Antennas Propag.*, vol. AP-23, no. 1, pp. 8–15, Jan. 1975.
[27] H. T. Friis, "A note on a simple transmission formula," *Proc. IRE*, vol. 34, no. 5, pp. 254–256, May 1946.
[28] T. S. Rappaport, *Wireless Communications: Principles and Practice*, vol. 2. Upper Saddle River, NJ, USA: Prentice-Hall, 1996.

KAPIL GANGWAR (Graduate Student Member, IEEE) received the B.Tech. degree in electronics and communication engineering from the Indian Institute of Technology-IIT (ISM), Dhanbad, India, in 2019. He is currently pursuing the M.Sc. degree with the Department of Electrical and Computer Engineering, University of Alberta, Edmonton, AB, Canada.

He has authored or coauthored over 11 research papers in international/national/journals/ conference proceedings. His current research interests include biomedical imaging, underground mine communication, dielectric resonator antenna, slot antenna, microstrip antenna, and RF energy harvesting circuits.

Mr. Gangwar was a recipient of the prestigious Alberta Innovates Graduate Student Scholarship and the University of Alberta Master's Recruitment Scholarship at the University of Alberta.

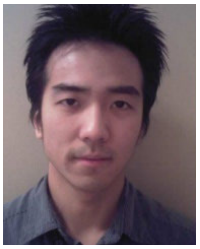

GARY CHIEN-YI CHEN received the B.Sc. degree in nanoengineering option from the Department of Electrical and Computer Engineering, University of Alberta, Edmonton, AB, Canada, in 2011.

From 2009 to 2011, he was a Research Student at the ECE Department, University of Alberta. His current research interests include the design and development of miniaturized Yagi class antennas for various wireless applications.

KEVIN KHEE-MENG CHAN (Member, IEEE) received the Ph.D. degree from the University of Alberta, Edmonton, AB, Canada, in 2014.

From 2001 to 2008, he was a Research Officer with the Institute for Infocomm Research, where he developed ultra-wideband (UWB) radar and RF identification (RFID) systems. He is currently a Postdoctoral Fellow with the University of Alberta, where he is involved with a microwave tomography system for medical imaging applications. His research interests include ultra-wideband (UWB) radar technology and passive microwave structures, such as filters, couplers, and antennas.

Dr. Chan was a recipient of the Tan Kah Kee Young Inventor's Award, in 2007, and the Alberta Innovates Graduate Student Scholarship, in 2011.

RAVI KUMAR GANGWAR (Senior Member, IEEE) received the B.Tech. degree in electronics and communication engineering from U. P. Technical University, Lucknow, in 2006, and the Ph.D. degree in electronics engineering from the Indian Institute of Technology (Banaras Hindu University), Varanasi, India, in 2011.

He is currently an Associate Professor with the Department of Electronics Engineering and the Associate Dean (Sponsored Research and Industrial Consultancy) at the Indian Institute of Technology (Indian School of Mines) Dhanbad, India. He has authored or coauthored over 100 research articles in reputed international journals and 80 papers in conference proceedings. His research interests include dielectric resonator antenna, microstrip antenna, and bio-electromagnetics. He is guided/guiding 15 Ph.D. and 19 M.Tech. students. He has completed/ongoing eight research and development projects (≈two crores rupees) related to dielectric resonator antenna and their applications from various funding agencies, like DRDO, SERB-DST, and ISRO.

Dr. Gangwar is a Senior Member of the Antenna and Propagation Society. He is a member of the Institution of Engineering and Technology (IET), U.K., a Life Member of the Institution of Engineers (IE), India, and a fellow of the Institution of Electronics and Telecommunication Engineers (IETE), India. He is also a member of the IETE Executive Council and Joint Regional Secretary at Ranchi Centre. He was a recipient of the INSA Visiting Scientist Fellowship and IETE Smt. Ranjana Paul Memorial Award for the year 2020. He is also an External Expert in the peer review committee of projects related to chaff application of the Defence Laboratory Jodhpur, DRDO. He is an Associate Editor of IEEE Access and *IET Circuits, Devices and Systems* journals. He is a Reviewer of IEEE Transactions on Antennas and Propagation, IEEE Antennas and Wireless Propagation Letters, *IEEE Antenna and Propagation Magazine*, *IET Microwaves, Antennas and Propagation*, *Electronics Letters* (IET), *Microwave and Optical Technology Letters*, and *Scientific Report*.

KARUMUDI RAMBABU (Member, IEEE) received the Ph.D. degree in electrical and computer engineering from the University of Victoria, Victoria, BC, Canada, in 2005.

He was a Research Member with the Institute for Infocomm Research, Singapore, from 2005 to 2007. Since 2007, he has been an Assistant Professor with the Department of Electrical and Computer Engineering, University of Alberta, Edmonton, AB, Canada, where he is currently a Professor. He is involved in oil well monitoring and pipeline inspection through wall imaging, vital sign monitoring, and biopsy needle guiding using ultra-wideband (UWB) radar systems. His current research interests include design and development of UWB technology and components and systems for various applications.

Dr. Rambabu was a recipient of the Andy Farquharson Award for excellence in graduate student teaching from the University of Victoria, in 2003, and the Governor Generals Gold Medal for the Ph.D. research, in 2005. He serves as an Associate Editor for the *IET Microwaves, Antennas and Propagation*.